

## Sedimentation Analysis of Polysaccharides

By Stephen E. Harding

UNIVERSITY OF NOTTINGHAM, DEPARTMENT OF APPLIED BIOCHEMISTRY  
AND FOOD SCIENCE, SUTTON BONINGTON, LE12 5RD U.K.

### 1. INTRODUCTION

Polysaccharides and related glycopolymers offer a unique challenge to analytical ultracentrifugation for two clear reasons. Firstly, there is a growing demand for basic solution biophysical information on these substances: molecular weights, molecular weight distributions, conformation, conformation distributions; information which analytical ultracentrifuge can, in principle, supply. This information is important for the understanding of for example the performance of so-called "commercial" polysaccharides in the food, drug and oil industries and for understanding the behaviour of glycopolymers such as mucus glycoproteins in health and disease.

The second reason is that despite the urgent requirement for this basic information, these macromolecules - compared to so-called 'well-behaved' macromolecules like many protein systems - are very difficult to analyse, because of their high thermodynamic non-ideality, their polydispersity (not only with respect to molecular weight but also in many circumstances with respect to composition) and, in several cases, their potential to self-associate in solution. Polysaccharides place therefore a considerable strain on available ultracentrifuge methodology and in many cases satisfactory information can only be achieved by combining results from the analytical ultracentrifuge with results from other techniques, notably light scattering, gel permeation chromatography and electron microscopy.

The aim of this Chapter is therefore threefold (i) to briefly survey the contributions that analytical ultracentrifugation has made to our understanding of polysaccharide systems; (ii) to indicate those advances in methodology of particular relevance to polysaccharides; (iii) to comment on possibilities for the future in the light of recent instrumental developments. We have also included a consideration of "mucopolysaccharides" *i.e.* mucus glycoproteins, since these share many of the characteristics (*e.g.* high viscosity and gel forming properties) of unconjugated polysaccharides, and indeed have a very high carbohydrate content (~80%). Two other important classes of glycopolymer - proteoglycans and hyaluronic acid - are considered in subsequent Chapters in this volume.

## 2. BASIC INFORMATION SOUGHT

### Molecular Weight and Heterogeneity

One of the most fundamental pieces of information describing a macromolecule is its molecular weight,  $M$ .  $M$  values for *polypeptides* can usually be evaluated without difficulty from chemical sequence information. For *polysaccharides* this is not the case, primarily due to their heterogeneity (polydispersity and self-association phenomena); an *average* molecular weight (usually the weight average,  $M_w$ ) is normally specified<sup>1</sup>. The ratios of the z-average molecular weight,  $M_z$  to  $M_w$  or  $M_w$  to the number average,  $M_n$  are used as indices for polydispersity.  $M_w$  is usually available to better than  $\pm 10\%$  from sedimentation equilibrium and  $M_n$  and  $M_z$  are also available but to a somewhat lower precision<sup>2</sup>.

Molecular weight *distributions* are a more representative indicator of heterogeneity. These can be obtained in principle at least from sedimentation equilibrium directly<sup>3</sup>; a much easier route is to combine gel permeation chromatography with sedimentation equilibrium<sup>4</sup>.

A good indication of *chemical heterogeneity* (e.g. purity) of a saccharide system can be provided by analytical isopycnic density gradient ultracentrifugation<sup>5</sup>.

### Gross Conformation

In general two levels of information are sought:

- (i) Delineation between the conformations represented by the extremes of the "Haug Triangle" (Fig. 1) *viz* compact sphere, rigid rod and random coil<sup>6,7</sup>. In general, most polysaccharides have conformations which - in the Haug representation - appear to lie between the extremes of rigid rod and random coil.
- (ii) More quantitative information. If the particle is a relatively rigid structure (as represented by side A of Fig. 1) this can be quantified in terms of either "bead"<sup>8</sup> or ellipsoid<sup>9</sup> models of the conformation. If the particle is more appropriately described by a rod, more detailed representations can be given in terms of length, diameter and mass per unit length<sup>10</sup>. If the particle conformation lies between rod and coil (side B), a measure of particle flexibility can be sought in terms of the ratio of the contour length to the persistence length<sup>10,11</sup>.

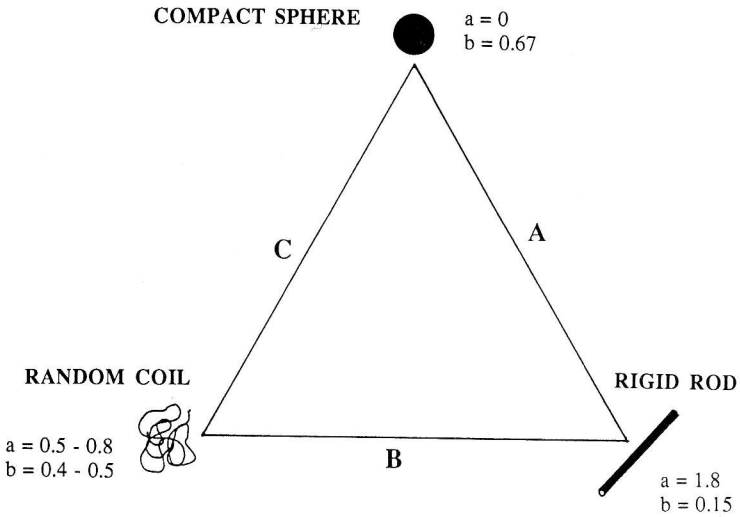


**Figure 1.** Haug Triangle representation of the gross conformation of macromolecules. The  $a$  and  $b$  are the exponents in the MHKS viscosity and sedimentation equations respectively (see ref. 6).

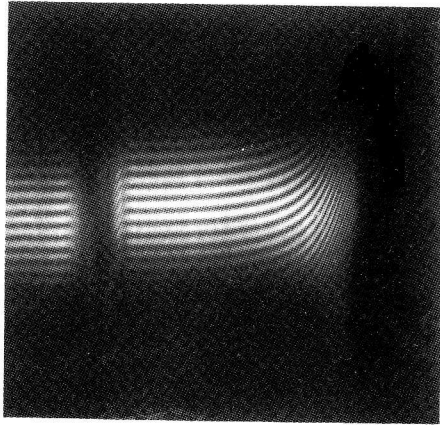


**Figure 2.** Rayleigh interference fringes from a low-speed sedimentation equilibrium experiment on a mucus glycoprotein or "mucopolysaccharide" from a chronic bronchitis patient ( $M \sim 6.0 \times 10^6$ ). Rotor speed = 2233 rev/min, loading concentration  $c_0 \sim 0.4$  mg/ml. Note the steep rise of the fringes at the cell base but finite slope of the fringes at the meniscus.

### 3. SEDIMENTATION EQUILIBRIUM

#### Optical System

The methodology behind recording solute distributions at sedimentation equilibrium and subsequent data capture and analysis has been dealt with earlier in this volume. Suffice to say here that most polysaccharides do not have a chromophore absorbing in the usable ultra-violet or visible spectrum and therefore to record solute distributions at equilibrium either Rayleigh or Schlieren optics have to be employed, both based on refractometric properties. Rayleigh interference is usually the optical method of choice<sup>12</sup> because of its greater sensitivity [concentrations as low as ~0.2 mg/ml can be used for cells of long (~30mm) optical path length] and an example of an equilibrium Rayleigh pattern is given in Fig. 2 [each solution fringe profile represents a plot of solute concentration relative to the meniscus]. For polysaccharide work the increased resolution in the Rayleigh fringes if a laser light source is used is particularly important.

#### Data Capture

Because of the demands on the precision and volume of data required for the analysis of polysaccharides, considerable attention has been recently afforded to the use of multiple-data-acquisition using automatic<sup>12</sup> or semi-automatic data capture procedures. We have been using for the last few years a semi-automatic procedure using a laser densitometer system to capture Rayleigh data off-line from photographic film<sup>13</sup>. Such data is then analysed *via* a frame-shift Fourier algorithm to yield the fringe concentration (relative to the meniscus) *versus* radial displacement. This data is then passed to a mainframe computer (in our case we use the IBM 3084/Q at Cambridge *via* a network link) for full molecular weight analysis.

#### Low Speed *versus* High Speed Sedimentation Equilibrium

An important choice has to be made prior to an ultracentrifuge run whether to attempt a meniscus depletion experiment or whether to use the more time-consuming low or intermediate speed method. The "high speed" meniscus depletion method<sup>14</sup> has been by far the most popular in biochemistry because it avoids the problem of evaluating the meniscus concentration or fringe number  $J_a$ . It also facilitates the evaluation of number average molecular weight data<sup>2</sup>. However for polysaccharides and mucus glycoproteins this method is not generally applicable because of the difficulty of obtaining proper depletion without losing optical registration of the fringes near the cell base (Fig. 2). A further difficulty in attempting meniscus-depletion conditions with polydisperse materials is that the effective thermodynamic second virial coefficient,  $B_{\text{eff}}$ , can be greatly enhanced<sup>15</sup>:

$$B_{\text{eff}} = B \left\{ 1 + \frac{\lambda^2 M_z^2}{12} + \dots \right\} \quad (1)$$

B being the "static" virial coefficient,  $\lambda = (1-\bar{v}\rho)\omega^2(b^2-a^2)/2RT$ ,  $\bar{v}$  the partial specific volume,  $\rho$  the solution density,  $\omega$  the angular velocity and  $a$  and  $b$  the radial positions at the cell meniscus and base respectively. This "speed dependence" effect can be minimised by using low speeds and short solution columns.

For polysaccharides, the low or "intermediate" speed method is therefore the more suitable: in this method the meniscus concentration remains finite and in general has to be found. A whole suite of procedures are available: Creeth and Pain<sup>16</sup> have given a comprehensive comparison of methods.

### Whole-cell Weight Average Molecular Weights: the $M^*$ Operational Point Average

Obtaining whole-cell (apparent) average molecular weight data for polysaccharides can be particularly difficult because of problems of obtaining estimates for the solute concentration at the meniscus *and* at the cell base. It is not usually sufficient to produce simply a plot of  $d\{\ln c(r)\}/dr^2$  (where  $c$  is the solute concentration at a given radial position  $r$ ) and "read off a slope", as is possible with 'well-behaved', monodisperse systems of many proteins. Furthermore, application of the widely used equation (see, *e.g.* ref. 16)

$$M_{w,app}^0 = \frac{1}{k} \left\{ \frac{c_b - c_a}{c_0 (b^2 - a^2)} \right\} \quad (2)$$

where  $k = (1-\bar{v}\rho)\omega^2/2RT$ ,  $c_0$  is the initial loading concentration (g/ml) and  $c_a$ ,  $c_b$  the concentrations at the cell meniscus and base respectively, or the related equation (in terms of the corresponding fringe number concentrations  $J_0$ ,  $J_a$  and  $J_b$  respectively)

$$M_{w,app}^0 = \frac{1}{k} \left\{ \frac{J_b - J_a}{J_0 (b^2 - a^2)} \right\} \equiv \frac{1}{k} \left\{ \frac{j_b}{J_0 (b^2 - a^2)} \right\} \quad (3)$$

where  $j_b$  is the fringe concentration (relative to the meniscus) at the cell base, is very difficult because of the form of the extrapolation of  $j(r)$  to the cell base; a further complication is that an accurate estimate for the initial loading concentration,  $J_0$ , is also required.

For polydisperse systems we have found an 'operational' point average molecular weight, the "star average"  $M^*$  particularly useful<sup>17</sup>. Although we have considered it in some detail earlier in this volume (Chapter 15), because of its particular usefulness for saccharide systems it will be constructive to briefly consider this again here but this time not in terms of reduced molecular weights. If we take the fundamental (differential) equation of sedimentation equilibrium in the form<sup>16,2</sup>

$$\frac{J(r)}{M_{n,app}(r)} - \frac{J_a}{M_{n,app}(a)} = 2k \int_a^r rJ \, dr \quad (4)$$

where  $M_{n,app}(r)$  and  $M_{n,app}(a)$  are the (apparent) number average molecular weights at a given radial position,  $r$  and the meniscus,  $a$  respectively, and then define an operational point average  $M^*(r)$  by the relation

$$M^*(r) = \frac{M_{n,app}(r) \cdot M_{n,app}(a)}{[M_{n,app}(a) \cdot J(r) - M_{n,app}(r) \cdot J_a]} \cdot j(r) \quad (5)$$

eq. (4) becomes:

$$\frac{j(r)}{M^*(r)} = kJ_a(r^2 - a^2) + 2k \int_a^r r j(r) dr \quad (6)$$

Eq. (6) has the limiting form

$$\lim_{r \rightarrow a} \frac{j(r)}{(r^2 - a^2)} = k \cdot M^*(a) \cdot J_a \quad (7)$$

A graph of  $j(r)/(r^2 - a^2)$  vs.  $(r^2 - a^2)^{-1} \times \int r j(r) dr$  therefore has a *limiting* slope of  $2kM^*(a)$  and an intercept  $kM^*(a) \cdot J_a$ ; hence  $J_a$  is determinable from the limiting slope and intercept. For ideal monodisperse systems both slope and intercept can be obtained without difficulty; for polydisperse and non-ideal systems, automatic data capture and multiple data analysis is particularly valuable for this purpose<sup>17</sup>. It is worth pointing out that Teller *et al.*<sup>18</sup> have considered other manipulations involving representations similar to eq. (6) for obtaining  $J_a$ . Other methods of obtaining  $J_a$  have been considered in detail by Creeth and Pain<sup>16</sup>. Once  $J_a$  has been found,  $M^*$  as a function of radial position can be defined.

A particularly useful property of the  $M^*$  function is that at the cell base ( $r=b$ ),

$$M^*(b) = M_{w,app}^0 \quad (8)$$

the (apparent) weight average molecular weight over the solute distribution<sup>17</sup>. The form of the extrapolation of  $M^*$  to the cell base is usually less severe than extrapolation of  $j$ ,  $J$  (or  $\ln J$ ) to the cell base to obtain  $M_{w,app}^0$  using eq. (3). Furthermore, an independent estimate of the initial loading concentration  $J_0$  is *not* required (although an estimate for  $J_a$  is required). Table 1<sup>17</sup> compares the performance of the two types of extrapolation procedure (*viz via* eq. (2) or eq. (8)) for several sets of synthetic data of relevance to polysaccharides.

**Table 1.** Comparison of  $M_w^0$  values obtained *via* the  $\ln J$  or  $M^*$  extrapolation procedures

	I	II	III	IV	V
$\ln J$	659000	4730000	2450000	2150000	499000
$M^*$	664000	4870000	2770000	2630000	500000
Theoretical	667000	4840000	3020000	3020000	500000

System I: Two component mixture,  $M_2 = 3M_1$ ;  $c_{0,2} = 0.167 c_{0,1}$ ;  $M_1 = 500000$ ;

System II: Very polydisperse (log normal,  $\sigma/\log M_w = 0.044$ ;  $M = 1.15 \times 10^6$ ;

System III: Isodesmic association,  $c = 1$ ,  $k = 2$  ( $M_1 = 500000$ );

System IV: As III but with fringe data with  $\pm 2 \mu m$  standard error;

System V: Single solute,  $M = 500000$ , fringe data with  $\pm 2 \mu m$  standard error.

From ref. 17

Two other useful properties of  $M^*$  have been given<sup>17</sup>:

- (i)  $M^*(a) = M_{w,app}(a)$ , the (apparent) point weight average at the meniscus;
- (ii)  $M^*(J=0) = M_{n,app}(a)$ , the apparent number average at the meniscus.

### Point Weight Average Molecular Weights

The differential form of the fundamental equation for sedimentation equilibrium is used<sup>16</sup>:

$$\frac{d \ln J(r)}{dr^2} = k M_{w,app}(r) \quad (9)$$

where  $M_{w,app}(r)$  is the (apparent) point weight average molecular weight. In our hands we find the Hildebrand sliding quadratic strip formulae as considered in Teller's article<sup>2</sup> of particular use, although some caution has to be expressed: if the strip width is too small (particularly for short fringe increments), the data can become too noisy; conversely, if too large, important trends in the data can be missed (for example genuine maxima or minima in  $M_{w,app}$  vs.  $c$  - or  $J$  - plots can be over-smoothed out).

### Number and z-averages

Until recently, attempts to obtain accurate estimates for both point and whole-cell number and z-averages have put an almost insurmountable strain on the quality of the Rayleigh fringe data unless heavy data smoothing is employed. However, with Rayleigh fringes generated by a laser light source and with the use of either on-line<sup>12</sup> or off-line<sup>13</sup> multiple data capture procedures, reasonable estimates can be obtained without too much difficulty. To obtain both point and whole cell number average molecular weight data sets, an estimate for the number average at the meniscus,  $M_{n,app}(a)$  is necessary<sup>2,16</sup>. As has been pointed out<sup>14</sup>, if the meniscus depletion method could be used, then the  $M_{n,app}(r)$  data would be much easier to obtain, but for saccharide systems this method is not always applicable as explained above. It has been suggested<sup>17</sup> that the identity  $M^*(J=0) = M_{n,app}(a)$  may be useful in this context; and it is worth remembering that solute distributions recorded using Schlieren optics yield z-average molecular weight data directly.

### Non-Ideality

For polysaccharides, non-ideality can be a particularly serious problem (Table 2<sup>19-27</sup>). Non-ideality affects colour the form of the dependence of the point average molecular weight on concentration or radial position; however, for many systems, measurement at a single finite, but low (0.2-0.5 mg/ml) concentration gives an estimate for the apparent  $M_w^0$  within a few percent of the true or "ideal"  $M_w^0$ . In extreme cases even a loading concentration as low as 0.2 mg/ml can lead to non-negligible underestimates for the true  $M_w^0$ : in Table 2, the term  $(1+2BMc)$ , with  $B$  the thermodynamic or "osmotic pressure" virial coefficient, represents the factor by which the apparent molecular weight measured at a finite concentration  $c=0.2$  mg/ml, underestimates the "true" or "ideal" molecular weight. Although in many cases the error is small, for saccharides such as alginates and hyaluronic acid, severe underestimates can result.

**Table 2.** Comparative non-ideality of polysaccharides.

	$10^{-6} \times M$ g/mol	$10^4 \times B$ ml.mol/g <sup>2</sup>	BM ml/g	<sup>a</sup> 1+2BMc	Ref.
Pullulan P5	0.0053	10.3	5.5	1.002	19
Pullulan P50	0.047	5.5	25.9	1.010	19
Xanthan (fraction)	0.36	2.4	86	1.035	20
$\beta$ -glucan	0.17	6.1	104	1.042	21
Dextran T500	0.42	3.4	143	1.057	22
Pullulan P800	0.76	2.3	175	1.070	19
Chitosan (Protan 203)	0.44	5.1	224	1.090	23
Pullulan P1200	1.24	2.2	273	1.109	19
Mucopolysaccharide <sup>b</sup>	2.0	1.5	300	1.120	24
Pectin (citrus fraction)	0.045	50.0	450	1.180	25
Scleroglucan	5.7	0.50	570	1.228	26
Alginate	0.35	29.0	1015	1.406	27

<sup>a</sup> Based on the lowest possible loading concentration (~0.2 mg/ml in a cell with a 30 mm path length centrepiece);

<sup>b</sup> Bronchial mucin CFPPI from a patient with cystic fibrosis.

In these cases, measurement of apparent  $M_{w,app}^0$ 's over a range of concentrations is necessary followed by an extrapolation to zero concentration<sup>19</sup> using an equation of the form<sup>1,7</sup>

$$\frac{1}{M_{w,app}^0} = \frac{1}{M_w^0} \{1 + (2B_{eff}M_w^0 - \bar{v})c\} \quad (10)$$

Fortunately, if solvent densities  $\rho_0$  are used instead of solution densities  $\rho$  for evaluating  $k$  in eq. (2), the  $\bar{v}$  term in eq. (10) drops out; this feature is implicit in the work of Fujita (pp. 284-285 of ref. 3) and stated explicitly by Wills and Winzor (Chapter 17 of this volume). Although this latter procedure yields an accurate  $M_w^0$ , caution has to be expressed when interpreting the second virial coefficient  $B$  from eq. (10) because of effects relating to eq. (1). In some extreme cases, third or even higher virial coefficient(s) may be necessary to adequately represent the data.

### Distributions of Molecular Weight

Direct inversions of solute distribution data to obtain molecular weight distribution information are generally intractable because of complications involving thermodynamic non-ideality<sup>3,28</sup>. The simplest procedure<sup>4</sup> avoiding these complications is to use sedimentation equilibrium *in conjunction with gel permeation chromatography* (GPC). Fractions of relatively narrow (elution volume) band width are isolated from the eluate and their  $M_w^0$  values evaluated by low speed sedimentation equilibrium in the usual way: the GPC columns can thereby be "self-calibrated" and elution volume values converted into corresponding molecular weights - a distribution can therefore be defined and in a way which avoids the problem of using inappropriate



"standards" for GPC: the value of Yphantis-style multi-channel cells for this purpose<sup>29</sup> is clearly indicated. This procedure has been successfully applied to dextrans, alginates and pectins: for pectins excellent agreement with analogous procedures involving classical light scattering coupled to GPC have been obtained (see, *e.g.* Fig. 3<sup>30</sup>).

#### 4. SEDIMENTATION VELOCITY

Some caution has to be expressed when interpreting sedimentation coefficient data for polysaccharides because of the strong concentration dependence of the sedimentation coefficient: this feature is considered in some detail in the following chapter in this volume by Lavrenko *et al.*<sup>31</sup>: extrapolation to zero concentration is therefore mandatory. Once found, the sedimentation coefficient,  $s_{20,w}^0$  and the concentration dependence regression coefficient,  $k_s$ , defined by the equation<sup>32</sup>:

$$\frac{1}{s_{20,w}} \approx \frac{1}{s_{20,w}^0} \{1 + k_s c\} \quad (11)$$

can be used for both molecular weight and conformational analysis.

#### Molecular Weight Analysis

The (weight-average) sedimentation coefficient can be combined *via* the well-known Svedberg equation<sup>33,34</sup> with the (z-average) translational diffusion coefficient (from sedimentation analysis<sup>35</sup> or from dynamic light scattering) to yield the weight average molecular weight<sup>36</sup>. This procedure has been used to obtain molecular weights of for example galactomannans<sup>37</sup>,  $\beta$ -glucans<sup>38,39</sup>, amylopectin<sup>40</sup>, alginate<sup>41</sup> and mucus glycoproteins<sup>42</sup>. Obtaining molecular weight *distributions* using sedimentation velocity is however not trivial. Although, after certain assumptions, estimates for distributions of sedimentation coefficients can be obtained<sup>43,44</sup>, obtaining corresponding distributions of diffusion coefficient (and at zero concentration), and then combining this data through the Svedberg equation *with* the sedimentation coefficient distribution data is to say the very least, unwieldy.

Nevertheless attempts have been made to obtain distributions of sedimentation coefficients for polysaccharides and, after assuming a particular conformation (sphere, random coil, rigid rod) and using the appropriate coefficients in the Mark-Houwink-Kuhn-Sakurada (MHKS) sedimentation equation (see *e.g.* ref. 7 and eq. (12) below), corresponding distributions of molecular weight have been inferred. This procedure has been followed for example for pig-gastric mucus glycoprotein<sup>45,46</sup>.

#### Conformational Analysis

**The Wales-van Holde Ratio** A useful guide to the gross conformation is the Wales-van Holde ratio<sup>47</sup> of the sedimentation concentration dependence regression coefficient,  $k_s$ , to the intrinsic viscosity,  $[\eta]$ . It is known empirically that this ratio has values of  $\sim 1.6$  for random coils and compact spheres and considerably lower for more extended conformations (see Lavrenko *et al.*<sup>31</sup> for a discussion on this). This ratio has been used as a guide to the conformations of a whole range of saccharides and Table 3<sup>19,21,30,40,50-53</sup> gives just a few representative examples.

**Table 3.** Values for  $k_s/[\eta]$  and the MHKS  $b$  coefficient for polysaccharides.

	$k_s/[\eta]$	$b$	Conformation	Ref.
Dextran fractions		0.44	Random coil	50
DIT-dextrans		0.56	Semi-flexible coil	51
Pullulans	~1.4	0.45	Random coil	19
$\beta$ -glucans	~0.4		Extended	21
Amylopectin <sup>a</sup>		1.45	Spheroidal	40
Alginates	~0.6		Extended	52
Pectins	~0.2	0.17	Rigid rod	30
Mucus glycoproteins	~1.5	~0.4	Random coil	53

All in aqueous solvents apart from "a" which is 90% DMSO, 10% H<sub>2</sub>O.

**Mark-Houwink-Kuhn-Sakurada (MHKS) Representations** We have indicated above that the (sedimentation) MHKS coefficients,  $K''$  and  $b$  in the equation

$$s_{20,w}^0 = K'' \cdot M^b \quad (12)$$

can be used to obtain estimates for the molecular weight directly from sedimentation coefficients. Like  $k_s/[\eta]$ , the MHKS exponent  $b$  (N.B. the exponent in eq. (12) is sometimes given as  $1-b$  - see ref. 31) is an indicator of gross conformation, having values of ~0.67, ~0.4-0.5 and ~0.15 for spheres, random-coils and rigid rods respectively (see, *e.g.*, ref. 7). MHKS  $b$  coefficients - obtained from double-log plots of  $s_{20,w}^0$  versus  $M_w^0$  (see, below) for a range of polysaccharides are also included in in Table 3. For polysaccharides of limited flexibility (this might apply, for example to short, polyanionic species), hydrodynamic methodology now permits the modelling of macromolecular conformation in terms of bead (*i.e.* multiple-sphere) models<sup>8,54</sup>, general triaxial ellipsoids<sup>9</sup> and rigid-rod models<sup>10</sup>. The latter has recently been used for example to estimate the mass per unit length of citrus pectins<sup>30</sup>.

**Worm-like Coil Models** This type of modelling possibly provides the best representation of polysaccharide conformation in solution, and covers the range from rigid rod to random coil. Garcia Molina *et al.*<sup>10</sup> have recently extended the earlier theory of Yamakawa and Fujii<sup>55,11</sup>.

## 5. ANALYTICAL ISOPYNIC DENSITY GRADIENT ULTRACENTRIFUGATION

W. Mächtle earlier in this volume (Chapter 10) has already stressed the power of analytical isopynic density gradient methods for characterising the chemical heterogeneity of synthetic polymer systems. This methodology, following the classical paper of Meselson *et al.*<sup>56</sup> has also been of considerable value for similar studies on systems of biological macromolecules, and indeed has been widely used for assaying the purity and composition of many systems of glycoconjugates, particularly glycoproteins (see, *e.g.*, ref. 5 and 57-60). It is however fair to say that its potential has thus far largely escaped the polysaccharide community.

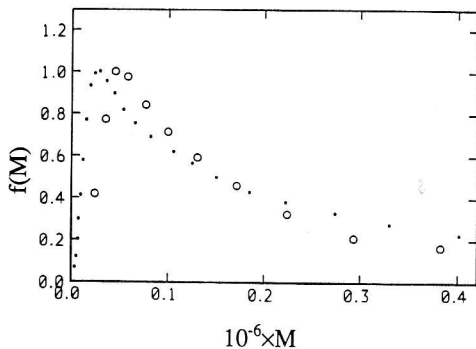


**Figure 3.** Distribution of molecular weight for Koch-Light citrus pectin determined by gel permeation chromatography with columns calibrated by absolute molecular weight measurements on pectin fractions by low speed sedimentation equilibrium (open circles) and total intensity or "classical" light scattering (filled circles). Reproduced, with permission, from ref. 30.

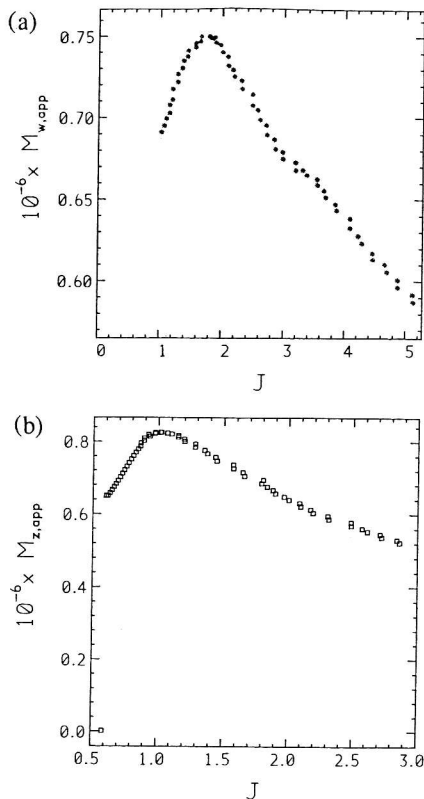


**Figure 4.** Plots of (apparent) point  $M_w$ ,  $M_z$  versus  $J$  for a purified guar preparation<sup>60</sup>. Rotor speed = 5200 rev/min; loading concentration,  $c^0 \approx 0.7$  mg/ml. The maxima in these plots are strongly symptomatic of a polydisperse but highly non-ideal system.

Very briefly, certain salts such as CsCl, CsBr, Cs<sub>2</sub>SO<sub>4</sub> and LiBr at sedimentation equilibrium distribute so that there is a significant distribution of solution density across the ultracentrifuge cell, a gradient which amongst other things will be a function of the salt, the rotor speed and the solution column length. A suspended macromolecule will, at equilibrium "band" at its isodensity point, which will either be at the meniscus, the base, or, if the density gradient has been appropriately chosen, somewhere between these two extremes. For example, the buoyant densities of proteins, polysaccharides and mucus glycoproteins are ~1.3 g/ml, ~1.6 g/ml and ~1.45 g/ml respectively.

There are three basic equations describing a density gradient (see, *e.g.* ref. 5). The first is:

$$\frac{d\rho}{dr} = \frac{\omega^2 r}{\beta} \quad (13)$$

where  $d\rho/dr$  is the density gradient and  $\beta$  is known as the "salt parameter" (not to be confused with the Scheraga-Mandelkern shape function).

The second gives the "iso-concentration" point,  $r_e$ , where the local density equals the initial density of the salt solution,  $\rho_e$ , for sector shaped cells (14a) and for cylinders (14b):

$$r_e = \sqrt{\frac{b^2 + a^2}{2}} \quad (14a)$$

$$r_e = \sqrt{\frac{b^2 + a^2 + ab}{3}} \quad (14b)$$

The third equation gives the density at a given radial position in the cell:

$$\rho = \rho_e + E(r-r_e) + E\left[\frac{1}{r_e} - EF\right]\frac{(r-r_e)^2}{2} \quad (15a)$$

where both

$$E \equiv \frac{\omega^2 r_e}{\beta} \quad (15b)$$

and

$$F \equiv \left[ \frac{d(\ln \beta)}{d\rho} \right]_{\rho=\rho_e} \quad (15c)$$

are independent of  $r$ . Values of  $\beta$  and  $F$  for the four salts commonly used in density gradient experiments are given in Table 4.

## 6. APPLICATIONS

We now survey some of the applications of sedimentation analysis to specific polysaccharide systems. This is by no means intended to be exhaustive, but rather to

illustrate the range of polysaccharide types analysed and the diversity of molecular weights, molecular weight distributions and conformations predicted.

### Dextrans

$M_w^0$  values for a whole series of commercial dextrans (a class of uncharged polysaccharides) have been estimated by sedimentation equilibrium and related techniques and classified in terms of "T" values (T500, T200, T50, *etc.*), the numerals representing the approximate molecular weight in kg/mol. These have subsequently been used as standard materials in, for example, gel permeation chromatography (GPC). One of the most widely studied has been T-500 dextran: good agreement has been obtained between sedimentation equilibrium and light scattering for 'whole distribution' weight average molecular weight determinations<sup>22,7</sup> and between GPC/sedimentation equilibrium and GPC/light scattering procedures for the determination of distributions of molecular weight<sup>61,62</sup>.

Double logarithmic representations of sedimentation coefficient *versus* molecular weight give an MHKS b coefficient of  $\sim 0.44$  suggestive of a random coil conformation<sup>50,51</sup>.

**Table 4.** Isopycnic density gradient equilibrium: values of the salt parameter,  $\beta$  and F as a function of density for four commonly used salts.

Salt	$\rho$ (g/ml)	$10^{-9} \times \beta$ $\text{cm}^5 \text{g}^{-1} \text{s}^{-2}$	F ml/g
CsCl	1.28*	1.582	-1.61
	1.30	1.533	-1.56
	1.40	1.334	-1.19
	1.41	1.319	-1.14
	1.45†	1.265	-0.93
	1.50	1.216	-0.64
CsBr	1.30	1.023	-1.97
	1.31*	1.003	-1.95
	1.40	0.852	-1.64
	1.50†	0.744	-1.04
Cs <sub>2</sub> SO <sub>4</sub>	1.24*	0.890	-2.57
	1.30	0.771	-2.15
	1.33†	0.726	-1.85
	1.50	0.650	+0.69
LiBr	1.30*	8.77	+0.39
	1.40	9.31	+0.79
	1.50†	10.25	+1.11

Adapted from ref. 5 and references cited therein. Values correct at a temperature of 25.0°C

\* Value regarded as characteristic of proteins

† Value regarded as characteristic of mucus glycoproteins.

The molecular weights of dextran *derivatives* have also been studied using sedimentation equilibrium, such as the cationic diethylaminoethyl (DEAE-) dextran<sup>63</sup> and di-iodotyrosine (DIT-) dextrans<sup>51</sup>. The value of  $\sim 0.56$  for the MHKS *b* coefficient for the latter is suggestive of a somewhat less flexible configuration for DIT-dextran compared to the native species<sup>51</sup>. A final interesting example for dextrans: advantage has been taken of the chromophore on "blue-dextran" to evaluate both sedimentation velocity<sup>64,65</sup> and sedimentation equilibrium behaviour<sup>65</sup> using the absorption optical system on the ultracentrifuge.

### Pullulans

Like dextrans, these are also now widely used as standard polysaccharides for GPC and other applications, and - like dextrans - have been classified in terms of their kg/mol molecular weights (P800, P200 *etc.*). Kawahara and co-workers<sup>19</sup> have determined values for  $M_w^0$ ,  $s_{20,w}^0$  and  $k_s/[\eta]$  for a whole series of fractions. As with dextrans, both the  $k_s/[\eta]$  and the MHKS *b* coefficient data<sup>19</sup> are consistent with a randomly coiled configuration in solution.

### Galactomannans

This is another class of uncharged polysaccharide, but unlike dextrans and pullulans, is much more difficult to characterise because of (i) greater difficulty in solubilisation in aqueous solvents and (ii) more extreme non-ideality behaviour<sup>66</sup>. Fig. 4 illustrates one example of this behaviour: the maximum in a plot of point average  $M_{w,app}$  (Fig. 4a) or  $M_{z,app}$  (Fig. 4b) *versus* (fringe) concentration, *J*, even at the relatively low initial loading concentration used ( $\sim 0.5$  mg/ml) is strongly symptomatic of a polydisperse but very non-ideal system (similar behaviour has been observed, *e.g.* for pig gastric mucus glycoprotein)<sup>67</sup>. Molecular weight values have been obtained for a series of locust bean gum galactomannans using both sedimentation equilibrium<sup>68</sup> and sedimentation/diffusion<sup>27</sup> and are in agreement with each other. Earlier light scattering procedures on these substances have given much higher molecular weights, a feature however probably ascribable to problems of clarification from supramolecular aggregates<sup>69</sup>. These difficulties appear to have now been circumvented with the advent of on-line GPC/light scattering procedures. Satisfactory agreement has for example now been achieved between sedimentation equilibrium and results from GPC/low angle laser light scattering (GPC/LALLS)<sup>70</sup> and the more recent on-line GPC/multi-angle laser light scattering (GPC/MALLS) for guar<sup>66</sup>. Sedimentation equilibrium has been used with viscometry to monitor the thermal degradation of commercial galactomannan samples<sup>52,71</sup>.

### $\beta$ -glucan

$\beta$ -glucans from barley<sup>21,38,39</sup> and wheat<sup>72,7</sup> have been studied. Woodward *et al.* have obtained estimates for  $M_w^0$  for two types of barley  $\beta$ -glucan ("clipper" and "commercial") from low speed sedimentation equilibrium; the values obtained ( $\sim 290000$  and  $\sim 160000$  respectively) are comparable with values obtained earlier using

sedimentation/diffusion on other preparations<sup>28,29</sup>. Results are also comparable for a series of wheat  $\beta$ -glucans also analysed by low speed sedimentation equilibrium<sup>72,7</sup>. Woodward *et al.*<sup>21</sup> also obtain relatively low values for  $k_s/[\eta]$  ( $\sim 0.3$  for clipper and  $\sim 0.5$  for commercial), which are suggestive of an extended rather than coiled or spherical conformation.

### Amylopectin

Unmodified amylopectins from starch are very difficult to obtain good solution data for because of their poor solubility in aqueous solvents. Amylopectins from wheat starch have been successfully solubilised in a mixture of 90% DMSO with 10% H<sub>2</sub>O<sup>73</sup> and Fronimos<sup>40</sup> and others have demonstrated the extreme concentration dependence of  $s_{20,w}$  in this solvent. Nonetheless, reasonably consistent estimates for  $s_{20,w}^0$  have been obtained:  $(206 \pm 13) S^{40}$ ,  $(230 \pm 16) S^{74}$  and  $(280 \pm 20) S^{75}$ .

Fronimos<sup>40</sup> has obtained an estimate for  $M_w^0$  of  $(85.0 \pm 5.0) \times 10^6$  using the sedimentation/diffusion (*viz* "Svedberg equation") method. Conformationally it appears from  $k_s/[\eta]$  ( $\sim 1.45$ ) to occupy a spheroidal rather than extended domain in this solvent<sup>40</sup>.

### Alginate

Alginates (from seaweed and some bacteria) are polyanionic co-polymers of mannuronic and guluronic acid residues. They are characterised by very high thermodynamic non-idealities (Table 1), and even at low loading concentrations ( $< 0.5$  mg/ml) the apparent  $M_w$  can be considerably lower than the infinite dilution value, even at relatively high ionic strength. Horton *et al.*<sup>76</sup> have observed that at concentrations  $> 0.5$  mg/ml, a third virial coefficient is necessary to account for the concentration behaviour. More precise estimates for the (ideal) molecular weight can be obtained by fitting molecular weights (rather than the reciprocals) directly to the concentration data (Fig. 5). Either way, results for *L. hyperborea* alginates from low speed sedimentation equilibrium are in general in good agreement with those from light scattering<sup>77,78</sup>. Wedlock *et al.*<sup>27,41</sup> have also obtained good agreement between the sedimentation/diffusion method and classical light scattering for a range of other alginates.

Conformationally, alginates appear from estimates for  $k_s/[\eta]$  ( $< 0.6$ ) to adopt an extended rather than spheroidal conformation in solution<sup>52</sup>.

### Pectins

These are another class of polyanionic polysaccharide and a range of pectins from different sources (usually from the cell walls of fruit) have now been relatively well characterised. The application of sedimentation procedures is particularly valuable here because of problems with light scattering through the persistent contamination of pectin preparations with microgels and other supramolecular particles that even the

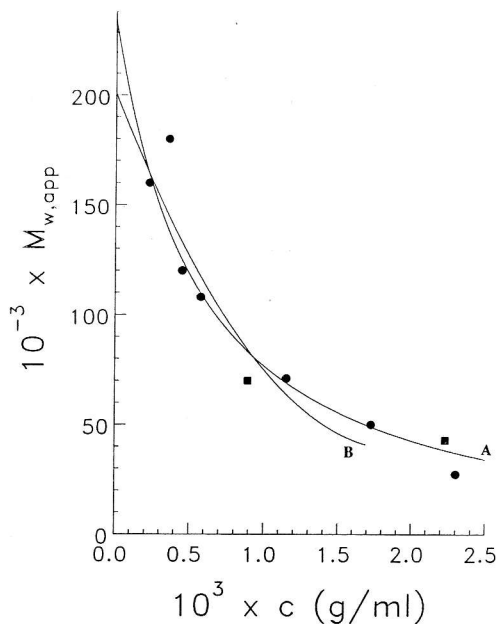


**Figure 5.** Plot of apparent molecular weight  $M_w$  versus concentration  $c$  for *L. hyperborea* alginate,  $I=0.3$ ,  $pH=6.8$ . Curve A is a weighted least squares fit to  $1/M_w$  versus  $c$  and curve B to  $M_w$  versus  $c$ . The different symbols (● and ■) correspond to different preparations. From ref. 76.

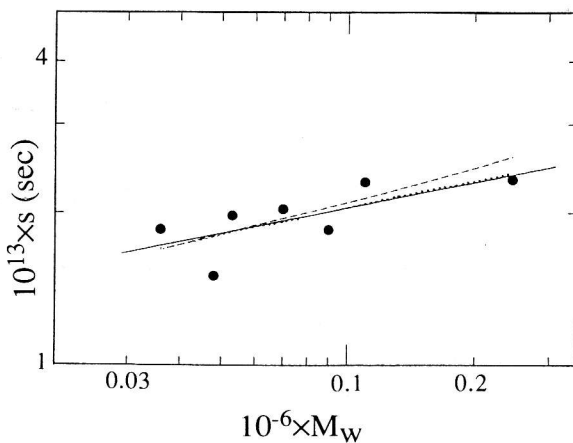


**Figure 6.** Double-logarithmic plot of  $s_{20,w}^0$  versus (whole-cell) weight average molecular weight values (from low speed sedimentation equilibrium) for citrus pectin fractions. Solid line corresponds to a fit of the data to the MHKS equation (eq. (12)). Dotted line (almost coincidental with the solid line) corresponds to a rigid rod model with mass per unit length  $430 \text{ g.mol}^{-1} \text{ nm}^{-1}$ . Dashed line corresponds to the fit to equations representing a worm-like coil with persistence length  $60 \text{ nm}$  and mass per unit length  $420 \text{ g.mol}^{-1} \text{ nm}^{-1}$ . (Reproduced with permission from ref. 30.)



most rigorous clarification procedures seem difficult to remove<sup>79</sup>. Low speed sedimentation equilibrium has been used to monitor the changes in the molecular weight of pectins from tomato cell walls during the ripening process (a change from large, relatively non-ideal to smaller, less non-ideal but more polydisperse systems has been observed<sup>80</sup>), changes which can be arrested to a significant degree on transforming the genes responsible for the production of galacturonase<sup>81</sup>. Citrus pectins have also been studied. The molecular weight distribution from the combined GPC/sedimentation equilibrium method (see §3 above) is in excellent agreement with that obtained from GPC/light scattering, after the latter had been corrected for the presence of microgels<sup>25</sup>. MHKS double-log  $s_{20,w}^0$  versus molecular weight (Fig. 6) and intrinsic viscosity versus molecular weight plots for a range of citrus pectin fractions are both consistent with a rod shape conformation ( $b=0.17\pm 0.10$ ) and also consistent with estimates for  $k_p/[\eta]$  ( $\sim 0.2$ ). A more detailed analysis has been given in terms of both rigid rod and wormlike coil models<sup>30</sup>. With the latter, the ratio of the contour length,  $L$ , to the persistence length,  $a$ , is consistent only with a rod shape conformation ( $L\sim a$ ).

### "Mucopolysaccharides": Mucus Glycoproteins

These are heavily glycosylated proteins ( $\sim 80\%$  CHO), of whose physical properties are more akin to polysaccharides than proteins<sup>76</sup>. Mucus glycoproteins from a wide variety of sources and molecular weights ( $\sim 0.5\text{--}16\times 10^6$ ) are thought to consist of the same hierarchical structure with basic units of  $M\sim 0.5\times 10^6$  covalently linked into a linear array to form, "subunits" of  $M\sim 2.5\times 10^6$ , and in turn linked *via* disulphide bridges into further linear arrays<sup>46</sup>. The role of the physical properties of these substances in health and disease is undisputed<sup>83</sup> but so far as their characterisation is concerned they pose some additional problems compared to "pure" polysaccharides in the sense that they are polydisperse in a "discrete sense" (through variability in the numbers of "basic units") as well as a "quasi-continuous" sense (through variability in the CHO side chain lengths<sup>46</sup>). Furthermore, because they are highly polydisperse not only with respect to *molecular weight* but also *density* (through variable CHO/peptide content), analytical density gradient procedures have been particularly fruitful and Creeth and co-workers have pioneered much of the methodology<sup>5,57-60</sup>. Fig. 7 shows examples of density gradient separations/simulations recorded using either absorption optics (on an MSE Centriscan) (Figs. 7a and 7b) or using conventional Schlieren optics on a Beckman Model E (Fig. 7c).

Distributions of molecular weights for pig gastric mucus glycoprotein have been inferred from an interesting approximation involving an axiom of indistinguishability between the effects of polydispersity or isodesmic self association phenomena in a *single* sedimentation equilibrium experiment<sup>85</sup>. The form of these distributions are in good agreement with that expected from sedimentation velocity<sup>45,46</sup> - the latter assuming a random coiled configuration<sup>46</sup> - and electron microscopy<sup>86</sup>. The "discrete" polydispersity in terms of variability of basic units has been studied using a direct iterative procedure for representing non-ideal polydisperse distributions at sedimentation equilibrium and satisfactory agreement with observations from electron microscopy has been obtained<sup>28</sup>.

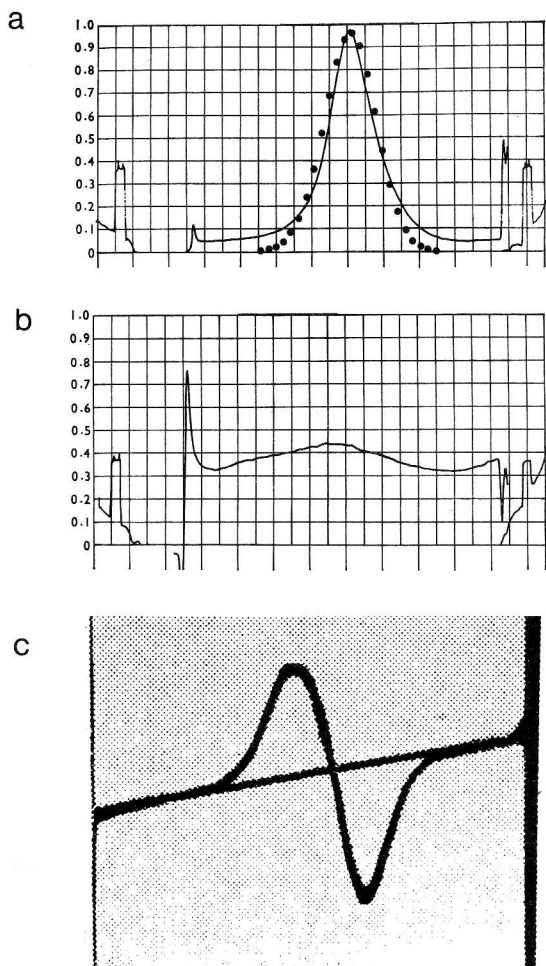


**Figure 7.** Isopycnic density gradient equilibrium of an ovarian cyst glycoprotein "603" (adapted from refs. 5 and 58).

(a) Fraction 50-60 ( $M_w=810,000$  g/mol). Distribution recorded using the absorption optical system of the MSE Centriscan. Salt:  $\text{Cs}_2\text{SO}_4$  ( $\rho_e=1.312$  g/ml). Rotor speed= $40,000$  rev/min at  $25.0^\circ\text{C}$ . Glycoprotein  $c^0=0.25$  ( $A_{280}$  units). The direction of the centrifugal field is from left to right. Plot is of  $A_{280}$  (absorbance at 280 nm) versus radial distance. Buoyant density  $\rho_0=1.310$  g/ml. The points  $\bullet$  correspond to an attempted simulation of the data in terms of the same buoyant density and a solvated molecular weight  $M_{s,app}=174,000$  g/mol.

(b) As (a) but in  $\text{CsCl}$  ( $\rho_e=1.507$  g/ml),  $c^0=0.33$ .

(c) Fraction 57 ( $M_w\sim 1.2\times 10^6$  g/mol). Distribution recorded using the (phase-plate) Schlieren optical system of the Beckman Model E. Salt:  $\text{Cs}_2\text{SO}_4$ . Rotor speed= $39460$  rev/min at  $25.0^\circ\text{C}$ . Glycoprotein  $c^0\sim 1.4$  mg/ml. Buoyant density,  $\rho_0=1.332$  g/ml. The background slope of constant gradient corresponds to the salt distribution.

Conformationally, despite their linear backbone, mucus glycoproteins from a wide variety of sources (bronchial, gastro-intestinal, ovarian, cervical) appear to adopt similar randomly coiled, spheroidal conformation in solution<sup>42</sup>; evidence for this has come from MHKS plots of  $\log s_{20,w}^0$  versus  $\log M$  and also double log MHKS plots of the translational coefficient and intrinsic viscosity versus molecular weight, supported by values for  $k_s/[\eta]$  of  $\sim 1.6$ <sup>53,86,87</sup>.

### ACKNOWLEDGEMENT

The initial help and encouragement of my mentor Dr. J.M. Creeth, who showed me ways of avoiding the minefield associated with these substances, is gratefully appreciated.

### REFERENCES

1. C. Tanford, 'Physical Chemistry of Macromolecules', Chapter 3, Wiley and Sons, New York, 1961.
2. D.C. Teller, *Methods Enzymol.*, 1973, 27, 346.
3. H. Fujita, 'Foundations of Ultracentrifuge Analysis', Chapter 5, Wiley and Sons, New York, 1975.
4. A. Ball, S.E. Harding and J.R. Mitchell, *Int. J. Biol. Macromol.*, 1988, 10, 259.
5. J.M. Creeth and J.R. Horton, *Biochem. J.*, 1977, 161, 449.
6. O. Smidsrød and I.L. Andresen, 'Biopolymerkjemi', 1979, Tapir, Trondheim.
7. S.E. Harding, K.M. Vårum, B.T. Stokke and O. Smidsrød, *Advances in Carbohydrate Analysis* (C. White ed.), 1991, 1, 63.
8. J. García de la Torre, in 'Dynamic Properties of Biomolecular Assemblies' (S.E. Harding and A.J. Rowe eds.), Chapter 1, Royal Society of Chemistry, Cambridge, 1989.
9. S.E. Harding, in 'Dynamic Properties of Biomolecular Assemblies' (S.E. Harding and A.J. Rowe eds.), Chapter 2, Royal Society of Chemistry, Cambridge, 1989.
10. M.C. Garcia Molina, M.C. Lopez Martinez and J. García de la Torre, *Biopolymers*, 1990, 29, 883.
11. H. Yamakawa and M. Fujii, *Macromolecules*, 1974, 7, 128.
12. T. Laue, Chapter 6, this volume.
13. A.J. Rowe, S. Wynne-Jones, D.G. Thomas and S.E. Harding, Chapter 5, this volume.
14. D.A. Yphantis, *Biochemistry*, 1964, 3, 297.
15. See e.g. H. Fujita, 'Foundations of Ultracentrifuge Analysis', pp. 290-293, Wiley and Sons, New York, 1975, for a discussion on this method.
16. J.M. Creeth and R.H. Pain, *Prog. Biophys. Mol. Biol.*, 1967, 17, 217.
17. J.M. Creeth and S.E. Harding, *J. Biochem. Biophys. Meth.*, 1982, 7, 25.
18. D.C. Teller, J.A. Horbett, E.G. Richards and H.K. Schachman, *Ann. N.Y. Acad. Sci.*, 1969, 164, 66.
19. K. Kawahara, K. Ohta, H. Miyamoto and S. Nakamura, *Carbohydr. Polym.*, 1984, 4, 335.

20. T. Sato, T. Norisuye and H. Fujita, *Macromolecules*, 1984, 17, 2696.
21. J.R. Woodward, D.R. Phillips and G.B. Fincher, *Carbohydr. Polym.*, 1983, 3, 143.
22. E. Edmond, S. Farquhar, J.R. Dunstone and A.G. Ogston, *Biochem. J.*, 1968, 108, 755.
23. R.A.A. Muzzarelli, C. Lough and M. Emanuelli, *Carbohydr. Res.*, 1987, 164, 433.
24. S.E. Harding, A.J. Rowe and J.M. Creeth, *Biochem. J.*, 1983, 209, 893.
25. G. Berth, H. Dautzenberg, D. Lexow and G. Rother, *Carbohydr. Polym.*, 1990, 12, 39.
26. D. Lecacheux, Y. Mustiere, R. Panaras and G. Brigand, *Carbohydr. Polym.*, 1986, 6, 477. See also T. Yanaki, T. Kojima and T. Norisuye, *Polym. J.*, 1981, 13, 1135.
27. D.J. Wedlock, B.A. Baruddin and G.O. Phillips, *Int. J. Biol. Macromol.*, 1986, 8, 57.
28. S.E. Harding, *Biophys. J.*, 1985, 47, 247.
29. D.A. Yphantis, *Ann. N.Y. Acad. Sci.*, 1960, 88, 586.
30. S.E. Harding, G. Berth, A. Ball, J.R. Mitchell and J. García de la Torre, *Carbohydr. Polym.*, 1991, 15, 1.
31. P.N. Lavrenko, K.J. Linow and E. Görnitz, Chapter 28, this volume.
32. H.K. Schachman, 'Ultracentrifugation in Biochemistry', Academic Press, N.Y., 1959.
33. T. Svedberg and K.O. Pedersen, 'The Ultracentrifuge', Oxford University Press, 1940.
34. C. Tanford, 'Physical Chemistry of Macromolecules', p. 380, Wiley and Sons, New York, 1961.
35. W.D. Comper and B.N. Preston, Chapter 23, this volume.
36. P.N. Pusey, in 'Photon Correlation and Light Beating Spectroscopy' (H.Z. Cummings and E.R. Pike, eds.), p. 387, Plenum Press, New York.
37. W.R. Sharman, E.L. Richards and G.N. Malcolm, *Biopolymers*, 1978, 17, 2817.
38. R. Djurtoft and K.L. Rasmussen, *Eur. Brew. Conv. Congr.*, p. 17, 1955.
39. O. Igarishi and Y. Sakurai, *Agr. Biol. Chem.*, 1965, 29, 678.
40. P. Fronimos, M.Phil. Thesis, University of Leicester, 1991.
41. D.J. Wedlock, B.A. Fasihuddin and G.O. Phillips, *Food Hydrocolloids*, 1987, 1, 207.
42. J.K. Sheehan and I. Carlstedt, in 'Dynamic Properties of Biomolecular Assemblies' (S.E. Harding and A.J. Rowe eds.), Chapter 17, Royal Society of Chemistry, Cambridge, 1989.
43. H. Fujita, 'Foundations of Ultracentrifuge Analysis', Chapter 3, Wiley and Sons, New York, 1975.
44. W.F. Stafford, Chapter 20, this volume.
45. R.H. Pain, *Symp. Soc. Exp. Biol.*, 1980, 34, 359.
46. S.E. Harding, *Adv. Carbohydr. Chem. and Biochem.*, 1989, 47, 345.
47. M. Wales and K.E. van Holde, *J. Polym. Sci.*, 1954, 14, 81.
48. J.M. Creeth and C.G. Knight, *Biochim. Biophys. Acta*, 1965, 102, 549.
49. P.Y. Cheng and H.K. Schachman, *J. Polym. Sci.*, 1955, 16, 19.

50. F.R. Senti, N.N. Hellman, N.H. Ludwig, G.E. Babcock, R. Tobin, C.A. Glass and B.L. Lamberts, *J. Polym. Sci.*, 1955, 17, 527.
51. N. Errington, S.E. Harding, E. Schacht and L. Illum, *Carbohydr. Polym.*, 1992, 17, in press.
52. A. Ball, Ph.D. Thesis, University of Nottingham.
53. J.K. Sheehan and I. Carlstedt, *Biochem. J.*, 1984, 217, 93.
54. J. García de la Torre, Chapter 18, this volume.
55. H. Yamakawa and M. Fujii, *Macromolecules*, 1973, 6, 407.
56. M. Meselson, F.W. Stahl and J. Vinograd, *Proc. Nat. Acad. Sci.*, 1957, 43, 581.
57. J.M. Creeth, K.R. Bhaskar, A.S.R. Donald and W.T.J. Morgan, *Biochem. J.*, 1974, 143, 159.
58. K.R. Bhaskar and J.M. Creeth, *Biochem. J.*, 1974, 143, 669.
59. J.M. Creeth, K.R. Bhaskar, J.R. Horton, I.R. Das, M.-T. Lopez-Vidriero and L. Reid, *Biochem. J.*, 1977, 167, 557.
60. J.M. Creeth, *Modern Problems in Paediatrics*, 1977, 19, 34.
61. A. Ball, S.E. Harding and N.J. Simpkin, in 'Gums and Stabilisers for the Food Industry' (G.O. Phillips, D.J. Wedlock and P.A. Williams, eds.), Vol. 5, pp. 447-450, IRL Press, Oxford, 1990.
62. Dawn F Application Note 7/8/88 No.3, Wyatt Technology Corp. (Santa Barbara USA), 1988.
63. M.T. Anderson, S.E. Harding and S.S. Davis, *Biochem. Soc. Trans.*, 1989, 17, 1101.
64. N. Errington, S.E. Harding and A.J. Rowe, *Carbohydr. Polym.*, 1992, 17, 151.
65. R. Acosta, B. Nyström and L.O. Sundelof, *Chemica Scripta*, 1981, 18, 7.
66. K. Jumel, J.R. Mitchell and S.E. Harding, in preparation.
67. J.M. Creeth and B. Cooper, *Biochem. Soc. Trans.*, 1984, 12, 618.
68. S.E. Gaisford, S.E. Harding, J.R. Mitchell and T.D. Bradley, *Carbohydr. Polym.*, 1986, 6, 423.
69. G. Robinson, S.B. Ross-Murphy and E.R. Morris, *Carbohydr. Res.*, 1982, 107, 17.
70. B.R. Vijayendran and T. Bone, *Carbohydr. Polym.*, 1984, 4, 299.
71. T.D. Bradley, A. Ball, S.E. Harding and J.R. Mitchell, *Carbohydr. Polym.*, 1989, 10, 205.
72. K.M. Vårum, S.E. Harding and O. Smidsrød, unpublished observations.
73. E. Dickinson, J. Lelievre, G. Stainsby and S. Wright, in 'Gums and Stabilisers for the Food Industry' (G.O. Phillips, D.J. Wedlock and P.A. Williams eds.), Vol. 2, pp. 447-450, Pergamon Press, Oxford, 1984.
74. J. Lelievre, J.A. Lewis and K. Marsden, *Carbohydr. Res.*, 1986, 153, 195.
75. W. Banks and C.T. Greenwood, 'Starch and its Components', Edinburgh University Press, 1975.
76. J.C. Horton, S.E. Harding, J.R. Mitchell and D.F. Morton-Holmes, *Food Hydrocolloids*, 1991, 5, 125.
77. A. Martinsen, G. Skjåk-Bræk, O. Smidsrød, F. Zanetti and S. Paoletti, *Carbohydr. Polym.*, 1991, 15, 171.
78. J.C. Horton, S.E. Harding and J.R. Mitchell, *Biochem. Soc. Trans.*, 1991, 19, 510.
79. G. Berth, *Carbohydr. Polym.*, 1992, in press.

80. G.B. Seymour and S.E. Harding, *Biochem. J.*, 1987, 245, 463.
81. C.J. Smith, C.F. Watson, P.C. Morris, C.R. Bird, G.B. Seymour, J.E. Gray, C. Arnold, G.A. Tucker, W. Schuch, S.E. Harding and D. Grierson, *Plant. Mol. Biol.*, 1990, 14, 369.
82. J.M. Creeth, *Br. Med. Bull.*, 1978, 34, 17.
83. F. Avery-Jones, *Br. Med. Bull.*, 1978, 34, 1.
84. See, for example, J.M. Creeth, K.R. Bhaskar, J.R. Horton, I. Das, M.T. Lopez-Vidriero and L. Reid, *Biochem. J.*, 1977, 167, 557.
85. D. Roark and D.A. Yphantis, *Ann. N.Y. Acad. Sci.*, 1969, 164, 245.
86. J.K. Sheehan, K. Oates and I. Carlstedt, *Biochem. J.*, 1986, 239, 147.
87. J.M. Creeth and C.G. Knight, *Biochem. J.*, 1967, 105, 1135.